OXIDATIVE DEAMINATION OF DIPEPTIDES BY SYNTHETIC MANGANESE OXIDE CHARACTERIZED BY HIGH RESOLUTION MASS SPECTROMETRY

A Thesis Presented to the Faculty of the Graduate School

of Cornell University

In Partial Fulfillment of the Requirements for the

Degree of Masters of Engineering

by

Johnny Huynh

April 2015

ABSTRACT

Manganese oxides (MnO_2) are ubiquitous in soils and have been implicated in the degradation of organic molecules including peptides, antibiotics, herbicides, and pesticides. In a previous study, glycine-glycine (gly-gly) was reacted with MnO_2 to yield Mn (II) and ammonia (NH_4^+), but the main degradation product was only qualitatively inferred. Using high resolution liquid chromatography-mass spectrometry (LC-MS), we identified and quantified the products formed following batch reactions with birnessite (δ-MnO_2) and dipeptides: gly-gly and alanine-glycine (ala-gly). After 24 h, the dipeptide concentration decreased by up to 70% for gly-gly and 40% for ala-gly (additional methyl group at the N-terminus α-carbon). Furthermore, we found that when gly-gly was in the presence of bicarbonate (HCO_3^-), degradation was impeded to only 10% after 24 h. The degradation products were identified with mass-to-charge ratio (*m/z*) of 130.049 and 144.065 for gly-gly and ala-gly respectively and are a result of N-terminal oxidative deamination at the α-carbon. These findings may be useful in elucidating the oxidized products of organic toxins with manganese oxides, as well as potentially producing a site specific aldehyde for synthetic chemistry purposes.

BIOGRAPHICAL SKETCH

Johnny Huynh earned his Bachelor of Science degree in Oceanography with a minor in Chemistry at the University of Washington in 2013. As an undergraduate, he was involved in paleoclimatology research with the Julian Sachs. After graduation, Johnny took a gap year and continued researching paleoclimatology in the Sachs Lab as an assistant researcher. He was also a lab technician in ecosystem research in the Simenstad Lab. In 2014, he joined the Biological and Environmental Engineering Masters of Engineering graduate program at Cornell University. Johnny's research was supervised by Dr. Ludmilla Aristilde.

ACKNOWLEDGEMENTS

I express gratitude to Dr. Ludmilla Aristilde for her mentorship, and guidance throughout the course of my Masters of Engineering program. Additionally, I thank my lab mates: Matt Kukurugya, David Flanelly, Hua Wei, and Ed Park, for their support and useful conversations. Also, a special thanks to Emily Hsieh, Jerry Du, Ted Bui, Jan Ramos, and Michael Duong for the encouragement and harsh criticism.

TABLE OF CONTENTS

LIST OF FIGURES

INTRODUCTION

Organic pollutants in soils are subject to oxidation by manganese oxides (MnO_2) (13). Due to its ubiquity in soils and high oxidation potential (5), the use of birnessite (δ-MnO_2) has been investigated for their redox catalyzed degradation of organic molecules such as pesticides (11), herbicides (2), and antibiotics (3). These studies provide evidence of degradation, but do not implicitly describe the evolution of the peptides present in the organics after oxidation. A study presented by Akram et al. (2011) (1) reported the generation of Mn (II), ammonia (NH_4^+), and a deaminated product following oxidation of glycine-glycine (gly-gly) by water-soluble colloidal MnO_2. However, the deaminated product was qualitatively inferred. In this paper, we quantitatively report on the degradation of model dipeptides: gly-gly (fig. 1A) and alanine-glycine (ala-gly) (fig. 1B), while also identifying the proposed deaminated products using high resolution liquid chromatography-mass spectrometry (LC-MS). Mass-to-charge (*m/z*) products of 130.049 and 144.065 for gly-gly and ala-gly respectively indicate N-terminal oxidative deamination at the α-carbon. Additionally, we tested our system in the presence of bicarbonate to observe the effect of alkalinity on the extent of dipeptide degradation. These findings will be useful in elucidating the oxidized products of organic contaminants, and could play a key role in wastewater treatment facilities or contaminated natural water systems (6).

Among other polymorphs of MnO_2, we chose birnessite for our experiments as it is the most commonly identified Mn oxide mineral in soils and geochemical environments (14). Birnessite is a layered phyllomanganate with edge-sharing MnO_6

octahedral sheets that have cation vacancies in which Mn (III) substitute for Mn (IV) due to structural defects, thereby introducing a negative structural charge. The negative charge is counterbalanced by solvated cations (Na^+, K^+) in the interlayer. Birnessite oxidizes through the reduction of Mn (IV) to Mn (II).

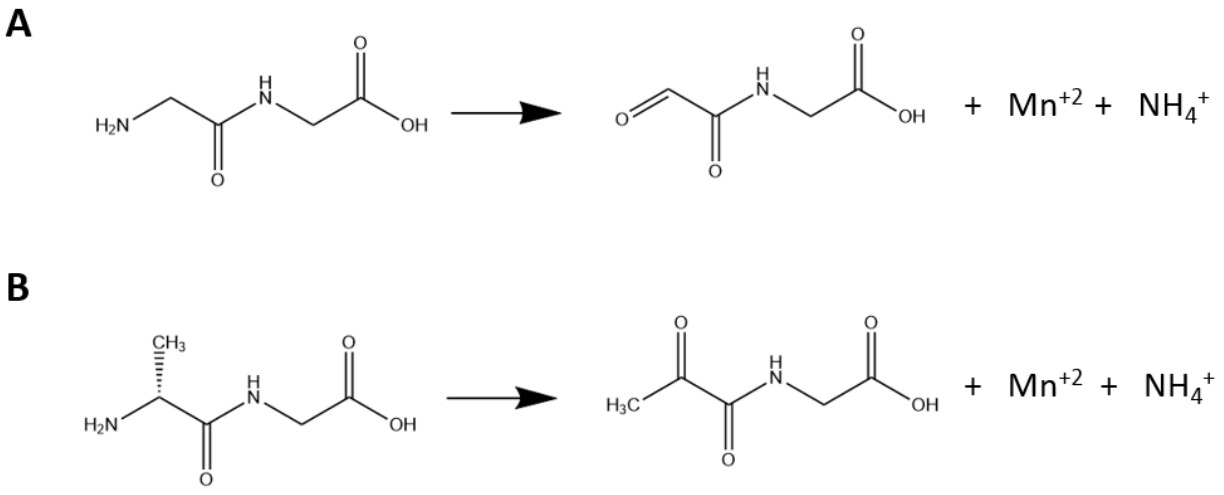

Fig. 1 Chemical structure of (A) gly-gly and *m/z* 130.049 and (B) ala-gly and *m/z* 144.065 after N-terminal oxidative deamination at the α-carbon.

MATERIALS

Chemicals

Sodium DL-lactate solution ($C_3H_5NaO_3$) 60% (w/w), and analytical grade (≥99.5% purity) potassium permanganate ($KMnO_4$), gly-gly, ala-gly, sodium bicarbonate ($NaHCO_3$), tributylamine, glacial acetic acid, hydrochloric acid, LC-MS grade methanol, and LC-MS grade water were obtained from Sigma Aldrich (St. Louis, MO) and Fisher Scientific (Hampton, NH) . For solutions, ultra-pure water (18.2 mΩ) from an EMD Millipore Q-Pod filtration system (Billerica, MA) was used.

METHODS

Synthesis of Birnessite

Birnessite was synthesized using a well characterized method (7). In a 250 mL Erlenmeyer flask we added 1 mL of 50% $C_3H_5NaO_3$ to 100 mL of 63.3 mM $KMnO_4$ and then stirred the solution for 2 h at 8 g until the purple color of the solution was completely reduced to dark brown flocculates. The precipitate was centrifuged at 1800 g for 10 min, followed by a decantation of the aqueous medium. The centrifugation and decantation were repeated 3 times by resuspending the solid in Milli-Q water to remove residual salts, and then lyophilized [Labconco FreeZone 4.5 L (Kansas City, MO)]. Finally, the solid was homogenized to a fine powder in a mortar and pestle.

Structural Characterization of Birnessite: X-Ray Diffraction (XRD) and Fourier Transform Infrared Spectroscopy (FT-IR)

The X-ray diffraction (XRD) characterization was conducted using a Bruker D8 Advance A25 (Billerica, MA). Birnessite was characterized at constant temperature (25 °C) and constant relative humidity (30%) and operated at 40 kV and 40 mA. The scanning parameters were 0.02° 2θ step size and 8 s as counting time per step over a 5-90° range (λ = 1.5418 Å). The three peaks present are characteristic of the main diffraction patterns of birnessite at 13, 40, and 65° (Appendix A). The diffraction chromatogram suggests crystalline disorder due to turbostratic stacking of the hexagonal and octahedral layers (8-9)

The infrared spectrum was obtained using a Bruker VERTEX 70 coupled with an HTS-XT High Throughput Screening eXTension (Billerica, MA) (Appendix B). The absorption peaks from 2500 cm^{-1} and 3700 and 1200-1700 cm^{-1} are characteristic of

H_2O in the interlayer space of the birnessite (10) while the other peaks between 400 and 800 cm^{-1} are defined by the MnO_6 octahedral framework (10). No adsorption bands from residual $C_3H_5NaO_3$ or $KMnO_4$ were detected.

Reaction Experiments with Birnessite

Batch adsorption experiments were conducted with 100 µM dipeptide solutions (gly-gly and ala-gly) and adjusted to pH 6 using hydrochloric acid. The dipeptide solutions were then reacted with 2 g L^{-1} and 10 g L^{-1} of birnessite respectively in 50 mL polyethylene centrifuge tubes for 24 h and prepared in triplicate. The mixtures were continuously agitated on a VWR incubating orbital shaker incubator (Radnor, PA) at 25 °C and covered in foil to prevent any effects from photo-oxidation. After 24 h, the birnessite suspension was filtered using a Pall 0.2 µm nylon membrane syringe filter (Port Washington, NY) for the supernatant. The dipeptide solutions were sampled at 0 and 24 h and then transferred to 300 µL Waters LC-MS vials (Milford, MA) where were immediately analyzed on the LC/MS. In order to test the effect of alkalinity, the same batch adsorption method was conducted, but under the presence of 2 mM $NaHCO_3$ in the background solution.

LC-MS Method

Both dipeptides and their degradation products were identified and quantified using a *Q Exactive* Hybrid Quadrupole-Orbitrap mass spectrometer coupled with a Thermo Scientific DionexUtiMate 3000 Rapid Separation UHPLC in negative electrospray ionization (ESI) mode. An Acquity UPLC BEH C18 column (100 mm × 2.1

mm, 1.7 µm particle size) was also used. The LC mobile phase consisted of a 97:3 LC-MS water to methanol with additions of 2.376 mL of 7.17 M tributylamine and 0.858 mL of 17.4 M acetic acid (solvent A), and LC-MS grade methanol (solvent B). A 25 min gradient separation with a flow rate of 0.180 mL min^{-1} was used in which solvent B increased from 0% to 20% after 5 min and kept for 5 min until increasing to 55% for 5 min, then increasing to 95% and kept for 5 min, and finally increasing solvent A to 100% for the remaining 5 min. Mass spectrometry parameters were set to a sheath, auxiliary, and sweep gas flow rate to 25, 8, and 5 respectively (arbitrary units), with a spray voltage of 3.3 kV, and a capillary and auxiliary gas heater temperature of 325 °C and 275 °C respectively.

Dissolved Mn Quantification

The amount of dissolved Mn (II) in the supernatant solution was quantified by oxidizing the colorless Mn (II) to a purple Mn (IV) and measuring the absorbance on an Agilent Cary 60 UV-Vis (Mattapoistt, MA) (15). In a 250 mL Erlenmeyer flask, 5 mL of the supernatant, 30 mL of Milli-Q water, and 10 mL of 9 M of phosphoric acid (H_3PO_4) were mixed together. Potassium periodate (KIO_4) was added in excess to ensure oxidation. Absorbance measurements were done at a wavelength of 525 nm.

$$2Mn^{+2} + 5KIO_4 + 3H_2O \rightarrow 2MnO_4^- + 5KIO_3 + 6H^+$$

RESULTS AND DISCUSSION

Reaction of Dipeptides with Birnessite

After 24 h, there was a 26.1% and 70.7% decrease in concentration with 2 g L^{-1} and 10 g L^{-1} of birnessite respectively (fig. 2A). For comparison, we performed the same experiment with ala-gly and observed a 6.64% and 36.8% decrease in concentration with 2 g L^{-1} and 10 g L^{-1} of birnessite respectively. The results were determined based on the peak area of the gly-gly and ala-gly at 0 and 24 h which both eluted out a retention time of 1.5 min (fig. 3A). From the results, the extent of oxidation is directly correlated to the amount of birnessite is added. However, less degradation was observed for ala-gly than gly-gly. In terms of structure, ala-gly has an additional methyl moiety at the α-carbon which explains tbe difference in degradation potential. Due to a size difference, it is possible that the methyl group introduces steric hindrance thereby contributing to a loss of available active sites on the birnessite. Saturation of the birnessite surface would render further oxidation and impede degradation.

Identification of Degradation Products

By comparing the control with the 24 h sample, we detected a degradation product at *m/z* = 130.049 (z=1) (fig. 3A and 4A) and is consistent with our hypothesis for oxidative deamination. The degradation product for gly-gly eluted out at a retention time of 7 min. Based on the later retention time, *m/z* = 130.049 is less polar than gly-gly. This is consistent with our findings as aldehydes are less polar than amine groups. For ala-gly, we detected a degradation product at *m/z* = 144.065 (fig. 3B and 4B). Based on the change in *m/z*, our hypothesis is confirmed for oxidative deamination. The degradation

product eluted out at a later retention time of 8 min which signifies a less polar compound. The oxidized product for ala-gly eluted out later than the product for gly-gly due to the extra methyl moiety which reduces polarity.

According to Levine et al, (1999) (12) and inferred by Akram et al, (2011), N-terminal oxidative deamination at the α-carbon was consistent with our results. However, it is important to note that N-terminal oxidative deamination in the former study only occurred when histidine was present in the second position. Akram reported oxidative deamination when glycine was at the second position, but did not verify if glycine was required for deamination to occur. Here, we observed deamination in both dipeptides with glycine at the second position.

Oxidation versus Adsorption

Despite a decrease in concentration of gly-gly and ala-gly with increasing amounts of birnessite, some material is lost due to sorption. Based on relative abundance (fig. 5), we determined the percent oxidized to be 69.5 and 64.9% for 2 g L^{-1} and 10 g L^{-1} of birnessite respectively with gly-gly (fig. 6). The remaining material is lost to sorption onto birnessite. This indicates that the decrease in dipeptide concentration is most facilitated by oxidation, and not through adsorption effects. Therefore, when adsorption is taken into account, the amount of possible degradation in gly-gly with 10 g L^{-1} of birnessite is actually 49.1% (down from 70.7%), and 23.9% in ala-gly (down from 36.8%).

Birnessite Dissolution

From the chemical equation in figure 1, the degradation of gly-gly using birnessite yields Mn (II) in solution. We saw a generation of 1.99 and 2.90 µM Mn (II) with 2 g L^{-1} and 10 g L^{-1} of birnessite respectively (fig. 7). The 31% increase in Mn (II) is consistent with results from figure 5 where relative abundances increased by ~30% following an increase of birnessite to 10 g L^{-1}. This indicates that there is approximately a 0.1 µM increase of Mn (II) for every g L^{-1} of birnessite in solution. Furthermore, this finding suggests that while the concentration of gly-gly can be oxidized by up to 70.7% (excluding effects from adsorption) with 10 g L^{-1} of birnessite, a very small percentage of the Mn (IV) in birnessite is actually being reduced to Mn (II).

Effect of Bicarbonate

We also tested the effect of increased alkalinity. We observed the concentration loss of gly-gly over 24 h by adding additions of 2 mM $NaHCO_3$ to our stock solution. Similar to conditions without sodium bicarbonate, we still observed a broad asymmetric peak with *m/z* 131.045 for gly-gly. After 24 h, there was a decrease of 3.56% and 12.9% for 2 g L^{-1} and 10 g L^{-1} respectively (fig. 8). The same degradation product for gly-gly was still observed for *m/z* 130.049. It is obvious that HCO_3^- impedes degradation, but the mechanism is not well understood in literature.

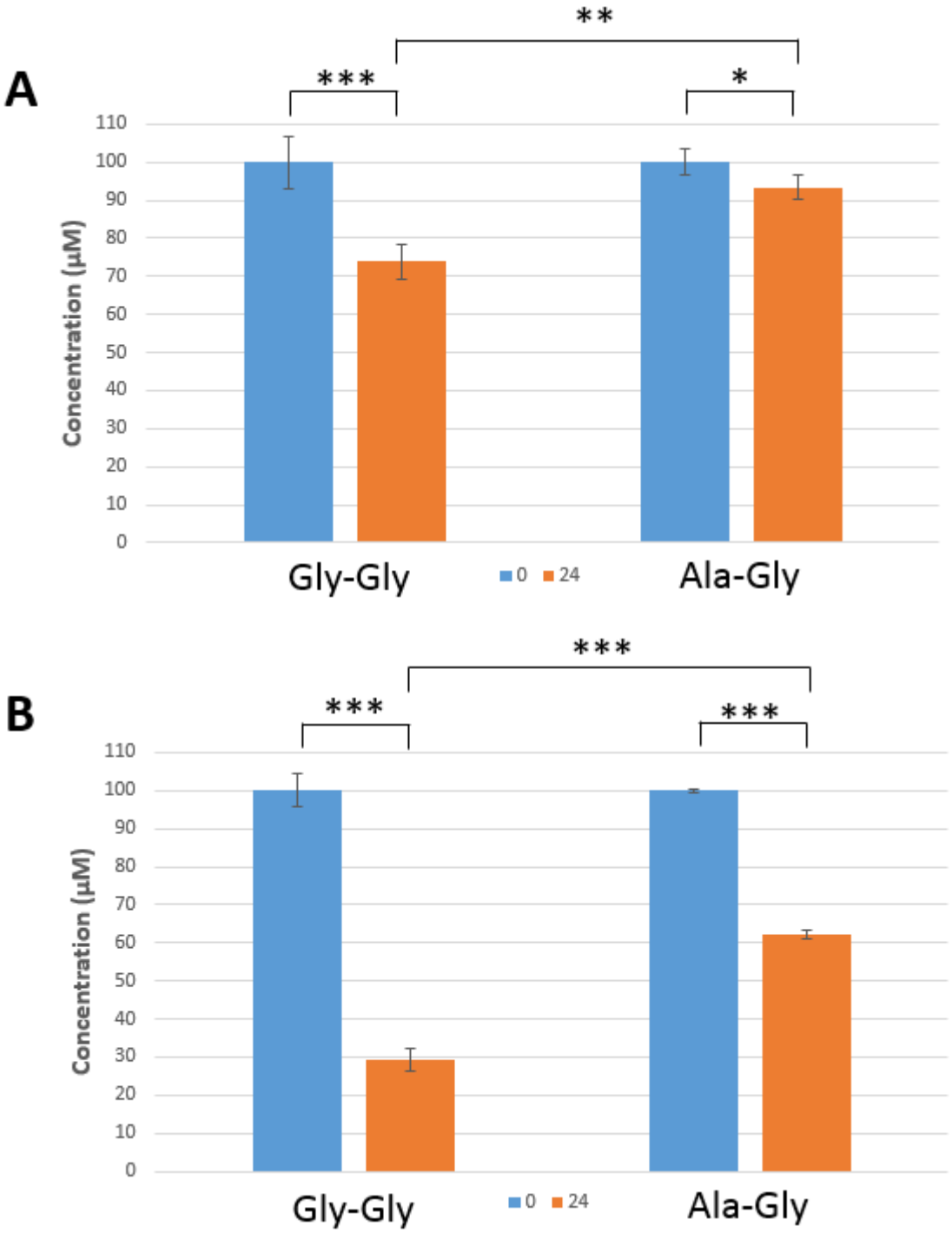

Fig. 2 Degradation of dipeptides gly-gly and ala-gly over 24 h with (A) 2 g L^{-1} and (B) 10 g L^{-1} of birnessite with no $NaHCO_3$ added. Control samples revealed no degradation over 24 h and negligible losses to the walls of LC/MS vials. Two-tailed unpaired *t* test analysis comparing gly-gly and ala-gly at 0 and 24 h (bottom statistics) and gly-gly versus ala-gly at 24 h (upper statistics): ***, $P < 0.001$; **, $P < 0.01$; *, $P < 0.05$.

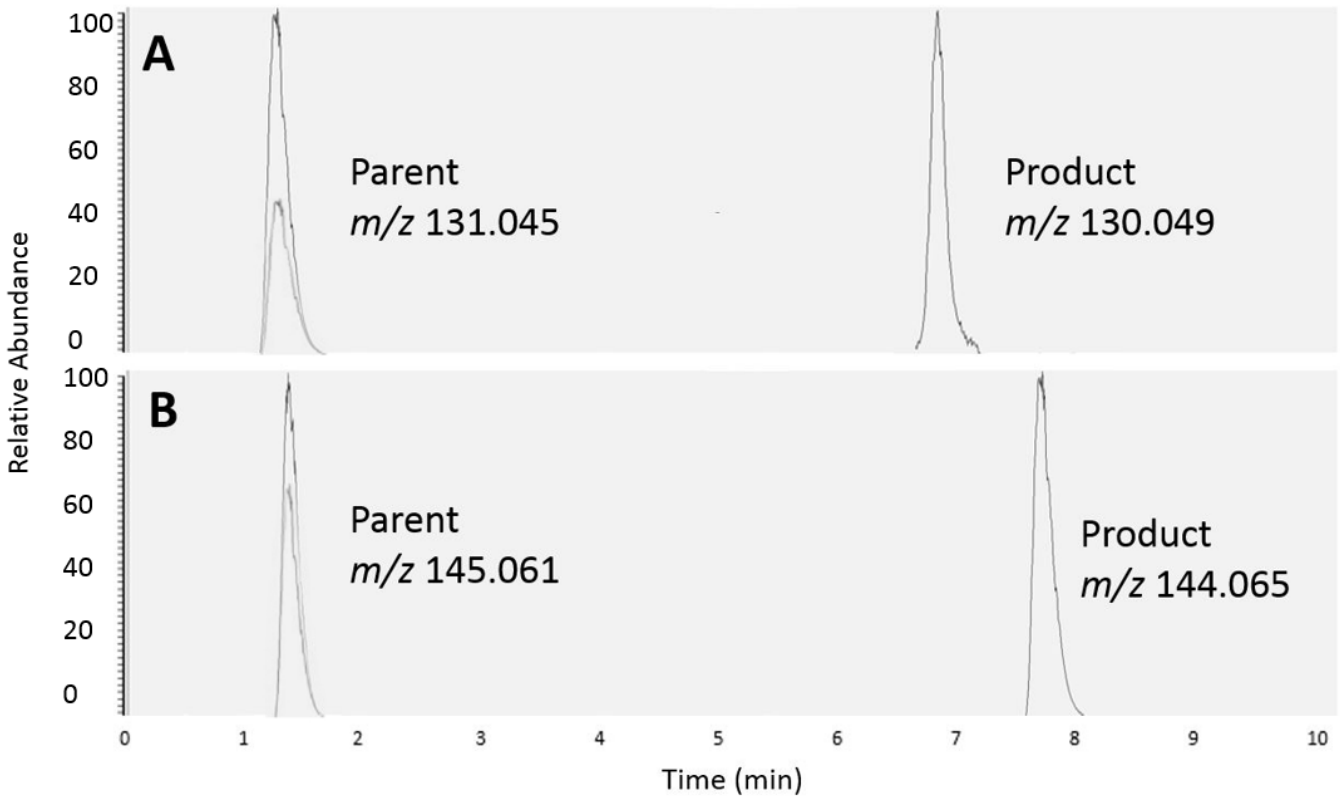

Fig. 3 LC-MS spectrum of (A) parental gly-gly and oxidized product *m/z* = 130.049, and (B) parental ala-gly and oxidized product *m/z* = 144.065 after 24 h. The parent peaks are referenced with the control.

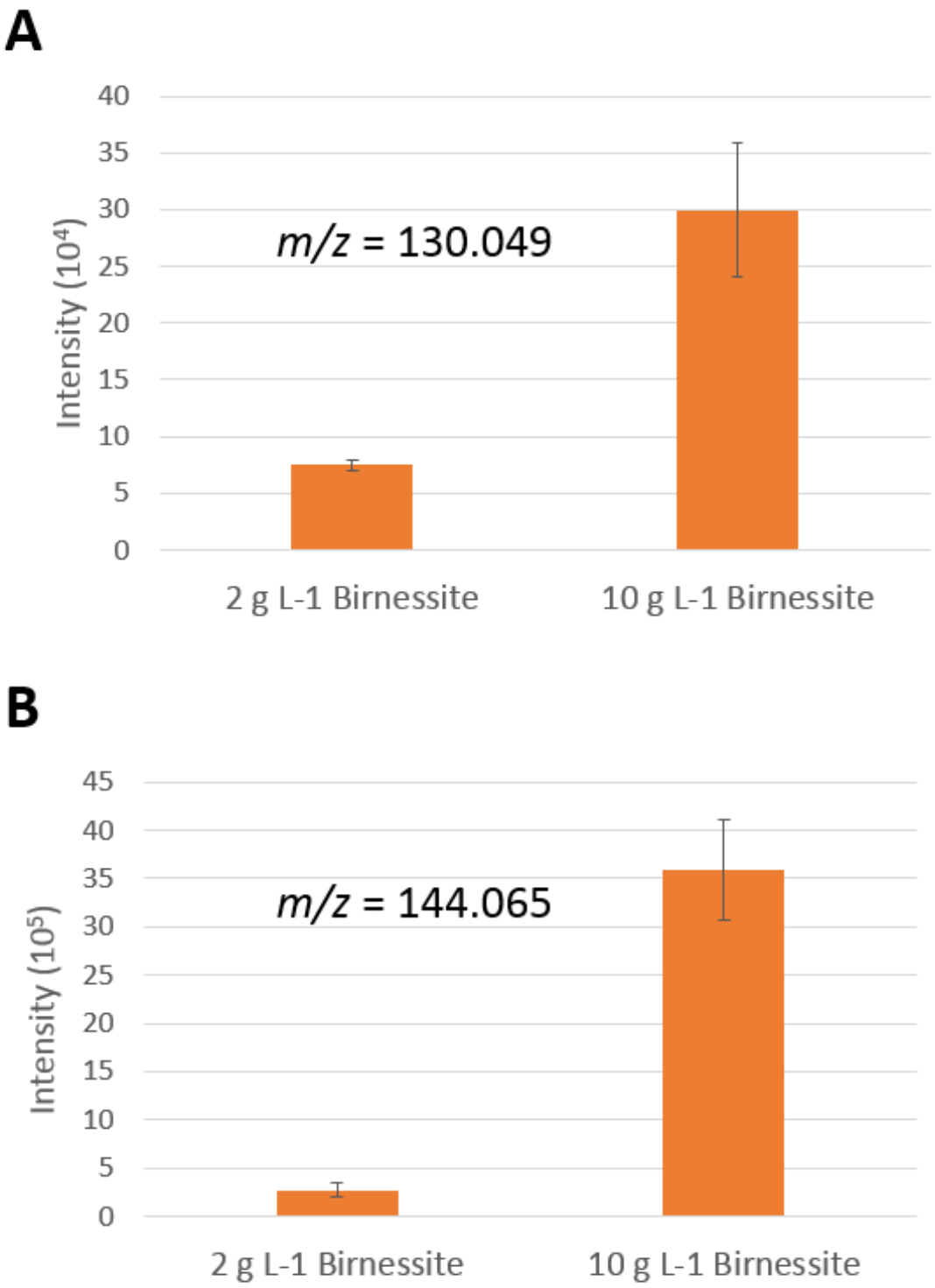

Fig. 4 Degradation product for (A) gly-gly with *m/z* 130.049 and (B) ala-gly with *m/z* 144.065 Intensity values for both degradation products at 0 h were not detected.

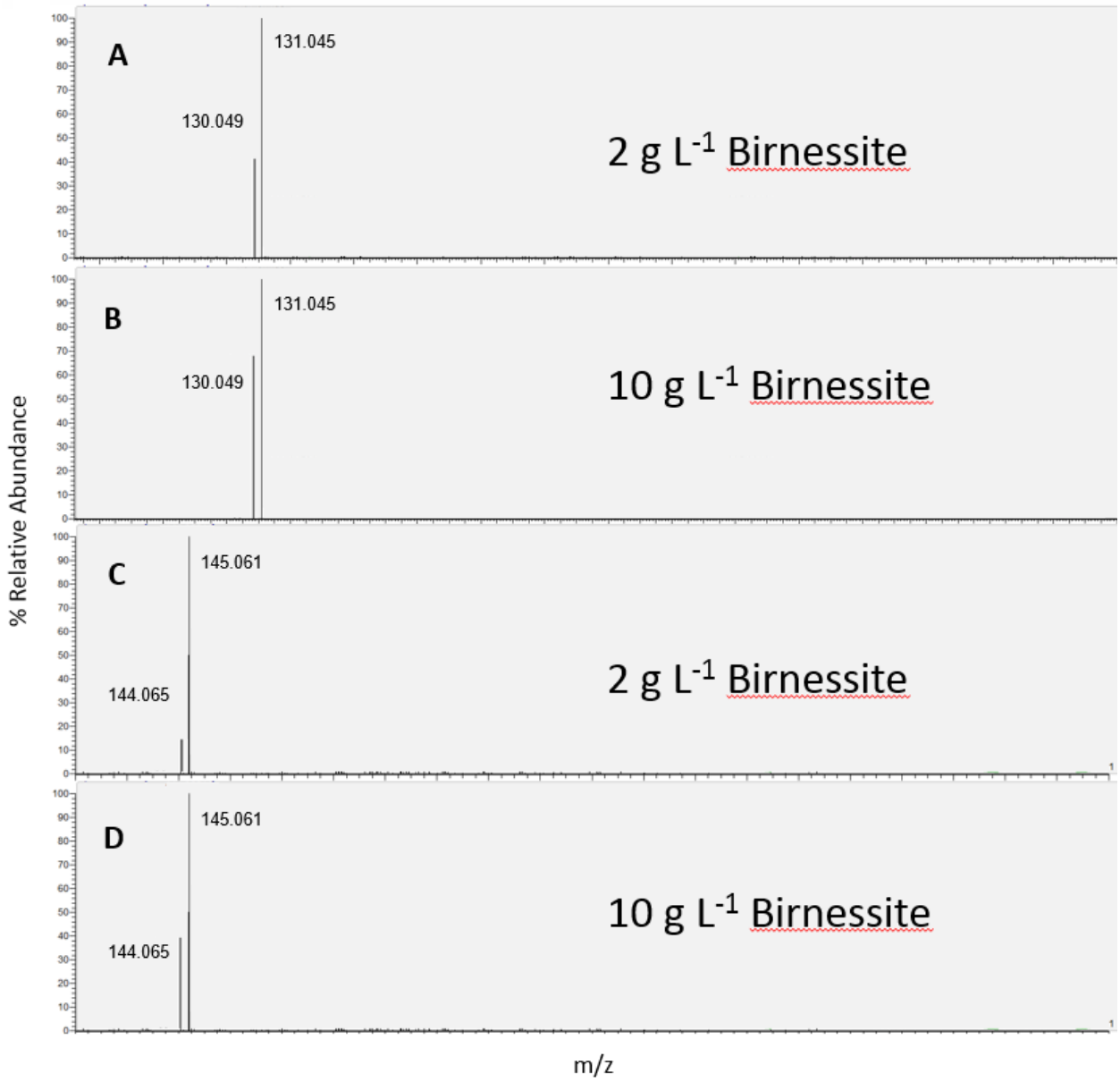

Fig. 5 Relative abundance of dipeptide and oxidized product after 24 h: (A) gly-gly and 2 g L^{-1} of birnessite, (B) gly-gly and 10 g L^{-1} of birnessite, (C) ala-gly and 2 g L^{-1} of birnessite, and (D) ala-gly and 10 g L^{-1} of birnessite

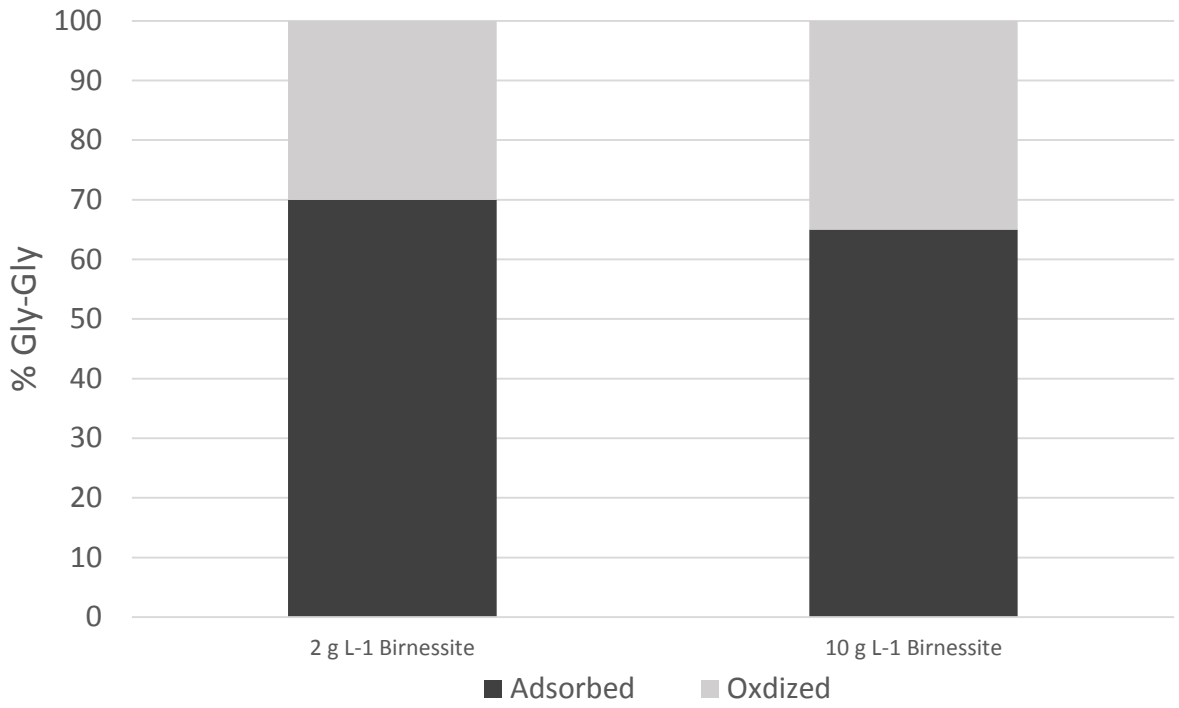

Fig. 6 Percent gly-gly oxidized versus adsorbed

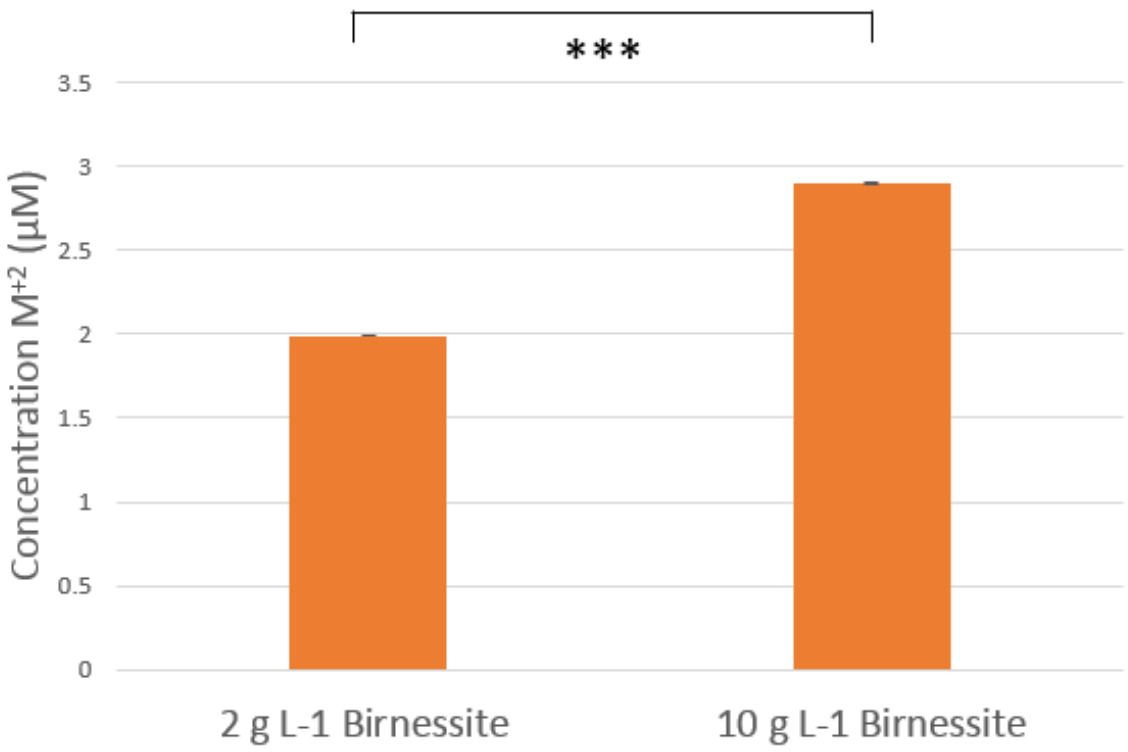

Fig. 7 Mn^{+2} concentration present in gly-gly supernatant solution after 24 h in the absence of $NaHCO_3$. Two-tailed unpaired *t* test analysis comparing 2 g L^{-1} and 10 g L^{-1}: ***, $P < 0.001$.

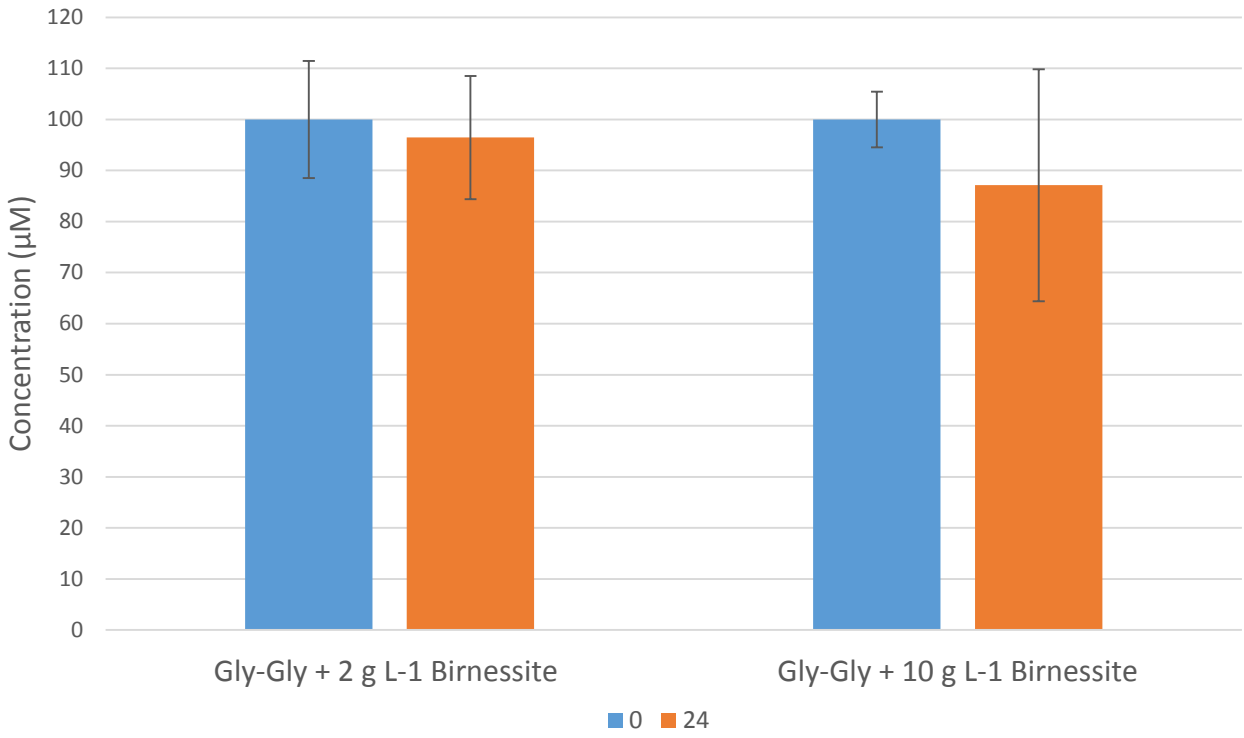

Fig. 8 Degradation of gly-gly over 24 h with 2 and 10 g L^{-1} of birnessite in the presence of HCO_3^- added for alkalinity. Control samples revealed no degradation over 24 h and negligible losses to the walls of LC/MS vials.

Conclusion

Birnessite has been shown to degrade dipeptides gly-gly and ala-gly over 24 h. It was also found that increasing the amount of birnessite greatly increased the degradation of both dipeptides, and it is likely that larger compounds could impede the amount of degradation by taking up available active sites. In the presence of HCO_3^-, it was also shown to impede degradation in gly-gly and ala-gly. Identification of degradation products revealed N-terminal oxidative deamination. The findings from this research provide a useful insight on predicting the oxidized compounds of organic contaminants for wastewater treatment purposes, as well as indicating a site specific aldehyde for synthetic chemistry purposes.

APPENDIX

A

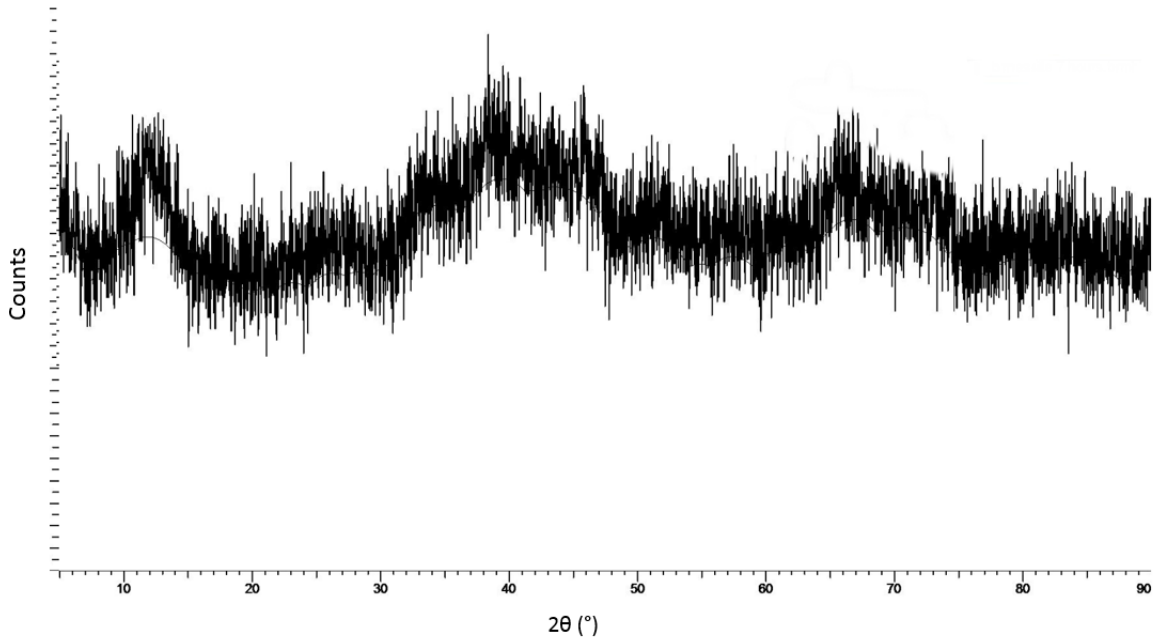

Appendix A XRD powder diffractogram of birnessite

B

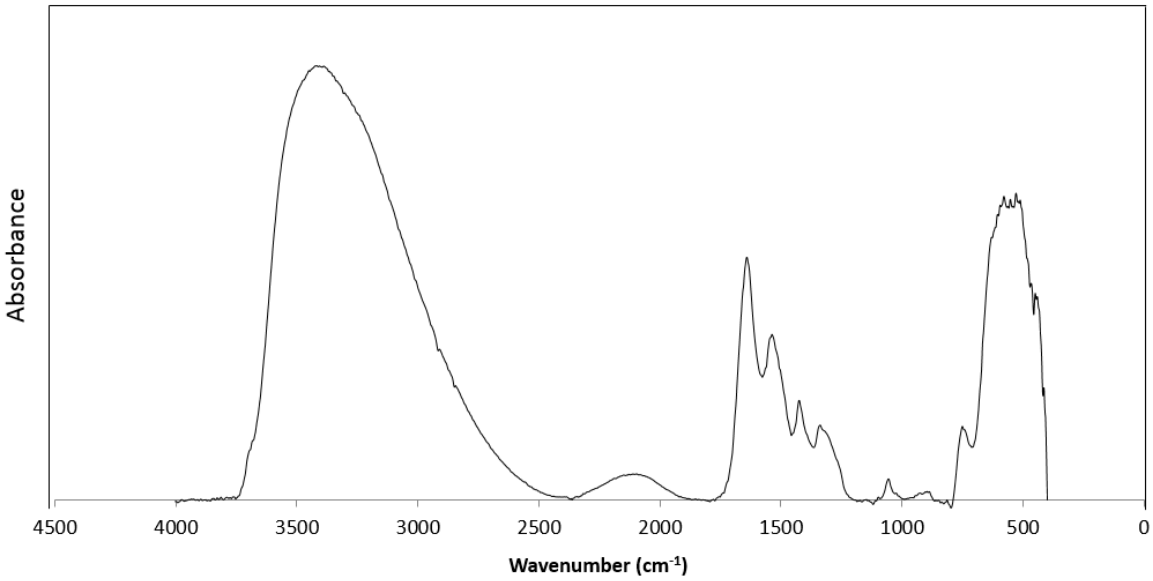

Appendix B FT-IR spectrum of birnessite

REFERENCES

1. Akram, M., Altaf, M., & Din, K. (2011). Oxidative degradation of dipeptide (glycyl–glycine) by water-soluble colloidal manganese dioxide in the aqueous and micellar media. Colloids and Surfaces B: Biointerfaces, 82, 217-223.
2. Barrett, K., & Mcbride, M. (2005). Oxidative Degradation of Glyphosate and Aminomethylphosphonate by Manganese Oxide. Environmental Science & Technology, 39(23), 9223-9228.
3. Kuan, W., Hu, C., Liu, B., & Tzou, Y. (2013). Degradation of antibiotic amoxicillin using 1×1 molecular sieve-structured manganese oxide. Environmental Technology, 34(16), 2443-2451.
4. He, Y., Xu, J., Zhang, Y., Guo, C., Li, L., & Wang, Y. (2012). Oxidative transformation of carbamazepine by manganese oxides. Environmental Science and Pollution Research, 19, 4206-4213.
5. Remucal, C., & Vogel, M. (2014). A critical review of the reactivity of manganese oxides with organic contaminants. Environ. Sci. Processes & Impacts, 16, 1247-1266.
6. Jiang, W., Long, C., Batchu, S., Gardinali, P., Jasa, L., Marsalek, B., Sharma, V. (2014). Oxidation of Microcystin-LR by Ferrate(VI): Kinetics, Degradation Pathways, and Toxicity Assessments. Environ. Sci. Technol, 48, 12164−12172-12164−12172.
7. Händel, M., Rennert, T., & Totsche, K. (2013). A simple method to synthesize birnessite at ambient pressure and temperature. Geoderma, 193-194, 117-121.
8. Drits, V.A., Silvester, E., Gorshkov, A.I.,Manceau, A., 1997. Structure of syntheticmonoclinic Na-rich birnessite and hexagonal birnessite. 1. Results from X-ray diffraction and selected-area electron diffraction. American Mineralogist 82, 9-10, 946-961.
9. Holland, K.L., Walker, J.R., 1996. Crystal structure modeling of a highly disordered potassium birnessite. Clays and Clay Minerals 44 (6), 744–748.
10. Potter, R.M., Rossman, G.R., 1979. Tetravalentmanganese oxides - identification, hydration, and structural relationships by infrared-spectroscopy. American Mineralogist 64, 11-12, 1199-1218.
11. Nasser, A., & Mingelgrin, U. (2014). Birnessite-induced mechanochemical degradation of 2,4-dichlorophenol. Chemosphere, 107, 175–179-175–179.
12. Levine, J., Etter, J., & Apostol, I. (1999). Nickel-catalyzed N-terminal Oxidative Deamination in Peptides Containing Histidine at Position 2 Coupled with Sulfite Oxidation. Journal of Biological Chemistry, 274(8), 4848-4857.
13. Semple, K., Morriss, A., & Paton, G. (2003). Bioavailability of hydrophobic organic contaminants in soils: Fundamental concepts and techniques for analysis. European Journal of Soil Science, 54, 809-818.
14. Mckenzie, R. (1971). The Synthesis of Birnessite, Cryptomelane, and Some Other Oxides and Hydroxides of Manganese. Mineralogical Magazine, 38, 493-502.
15. “Measuring Manganese Concentration Using Spectrophotometry”. Santa Monica College. 2011: 1-8.